Design of Spatial Fast- and Slow-Time Waveforms and Receive Filter for MIMO Radar Space-Time Adaptive Processing

Chunxuan Shi, Yongzhe Li, and Ran Tao
School of Information and Electronics, Beijing Institute of Technology, Beijing 100081, China
Emails: chunxuanshi@bit.edu.cn, lyz@ieee.org/yongzhe.li@bit.edu.cn, rantao@bit.edu.cn

***Abstract*—In this paper, we study the joint design of transmit waveforms and receive filter for the multiple-input multiple-output (MIMO) radar with space-time adaptive processing (STAP), wherein the complex environment that involves both clutter and jamming signals is considered. We choose to simultaneously design both the fast-time waveform and slow-time coding among transmitted pulses, together with the design of adaptive processing at receiver, which therefore leads to a three-dimensional STAP for MIMO radar. Specifically, we maximize the signal-to-jammer-plus-clutter-plus-noise ratio at the output, and meanwhile, we ensure the constant-modulus and similarity constraints for the waveform transmission. Based on this, we formulate the joint design as a non-convex optimization problem, and then recast it into a form that allows the application of alternating direction method of multipliers to find its solution. Moreover, we propose an algorithm with fast convergence speed for the conducted design, whose effectiveness is verified by simulations.**

***Index Terms*—Joint design, MIMO radar, spatial fast and slow-time waveforms, space-time adaptive processing (STAP).**

I. Introduction

As a research field of significant interest, the multiple-input multiple-output (MIMO) radar has attracted considerable attention in recent years [1]–[6]. It has been verified by various research to enable superiorities such as improved parameter identifiablity and angular resolution [1], increased upper limit on the number of resolvable targets [1], extended array aperture by virtual array [3], etc. In recent years, these advantages have stimulated the utilization of space-time adaptive processing (STAP) technique in MIMO radar in order to suppress both clutter and hostile jamming signals [6]. Compared to the conventional STAP in phased-array radar, the MIMO radar STAP has been proved by the research of ground moving target indication to have the ability of attaining lower minimum detectable velocity, or in other words, the narrower clutter/jamming mitigation notch versus Doppler frequencies [6]–[8]. However, in the context of complex environment such as the presence of diffuse jamming via multi-path propagation coexisting with clutter signals, the three-dimensional (3D) STAP is typically required for the MIMO radar [7].

There have been recent research focusing on developing strategies at the transmitting end of MIMO radar [9]–[11]. By means of devising correlated waveforms [9], waveform covariance matrix [10], or transmit beamspace matrix [11], these strategies allow to achieve desired properties such as arbitrary beampattern (possibly flat) over a certain spatial sector, reduced sidelobe levels of waveforms, or improved transmit coherent processing gain. Considering that these properties may benefit MIMO radar STAP from the perspective of output signal-to-jammer-plus-clutter-plus-noise ratio (SJCNR), and conventional MIMO radar assumes fixed waveforms that are non-adaptive, it is worth studying the joint design of transmit waveforms and receive filter for MIMO radar STAP. To distinguish from the existing works on transmit waveform and receive filter design that focus either on fast- or slow-time waveforms [12]–[17], it is worth designing simultaneous waveform transmission in both the fast- and slow-time domains.

In this paper, we study the problem of joint waveform transmission and receive filter design for the MIMO radar STAP. Since the complex environment that simultaneously involves clutter and jamming signals is present, we therefore devise both fast and slow-time waveform transmissions for the joint design. Our goal is to improve the clutter and jammer suppression performance for the three-dimensional (3D) STAP of MIMO radar. To be specific, We maximize the SJCNR at the output of receiver, and meanwhile, we guarantee the constant-modulus and similarity constraints to enable desirable properties such as spectral agility for the transmitted waveforms. Based on this idea, we formulate the design as a non-convex optimization problem, and then reformulate it into a proper form which supports the use of alternating direction method of multipliers (ADMM) for solutions. To this end, we elaborate a gradient-based Lagrangian for the ADMM, by which we seek to find solutions to the design problem via iterations. A closed-form solution is attained at each iteration, which finally leads to the development of an algorithm for the joint design. Simulation results show the effectiveness of our proposed algorithm, wherein fast convergence speed and simultaneously good similarity to desired waveforms are achieved.

Notations: We use bold upper case, bold lower case, and italic letter to donate matrices, column vectors, and scalars, respectively. Notations $(\cdot)^{\mathrm{T}}$, $(\cdot)^{\mathrm{H}}$, $\otimes$, $\odot$, $\mathfrak{D}(\cdot)$, $\mathrm{vec}(\cdot)$, $\mathbb{E}\{\cdot\}$, $|\cdot|$, and $[\cdot]_{i,j}$ are respectively the transpose, conjugate transpose, Kronecker product, Hadamard product, diagonalization, column-wise vectorization, expectation, modulus, and the (i,j)-th element of a matrix. In addition, $\mathbb{C}$ and $\mathbf{I}_P$ stand for the

This work was supported in part by the National Natural Science Foundation of China (NSFC) under Grants 61901041, 62171029, and U21A20456.

complex field and the $P \times P$ identity matrix, respectively.

II. Signal Model and Problem Formulation

Consider an airborne colocated MIMO radar with M transmit and N receive antenna elements. Both the transmit and receive arrays are closely spaced so that they share an identical spatial angle for a far-field target. We assume that the MIMO radar transmits a burst of L pulses in one radar coherent processing interval (CPI). The transmit waveform matrix in the fast-time domain is denoted by $\mathbf{S} \triangleq [\mathbf{s}_1, ..., \mathbf{s}_M]^{\mathrm{T}} \in \mathbb{C}^{M\times P}$, where P is the length of each waveform launched at a certain transmit antenna element. The slow-time waveform, denoted as a vector given by $\mathbf{u} \in \mathbb{C}^{L\times 1}$, is used for inter-pulse modulation. By stacking all the slow- and fast-time samples at the receiving end, the observation of a target located at the spatial angle θ_{t} with normalized Doppler frequency f_{t} can be expressed as

$$\mathbf{y}_{\mathrm{t}}(\mathbf{u},\mathbf{S}) = \alpha_{\mathrm{t}}(\mathbf{d}(f_{\mathrm{t}}) \odot \mathbf{u}) \otimes (\mathbf{S}^{\mathrm{T}}\mathbf{a}(\theta_{\mathrm{t}})) \otimes \mathbf{b}(\theta_{\mathrm{t}}) \quad (1)$$

where α_{t} is the complex reflection coefficient of the target, $\mathbf{a}(\theta_{\mathrm{t}})$, $\mathbf{b}(\theta_{\mathrm{t}})$, and $\mathbf{d}(f_{\mathrm{t}})$ are respectively the transmit, receive, and Doppler steering vectors of the target given as follows

$$\mathbf{a}(\theta_{\mathrm{t}}) \triangleq [1, e^{-j2\pi d_{\mathrm{T}} \sin\theta_{\mathrm{t}}/\lambda}, ..., e^{-j2\pi(M-1)d_{\mathrm{T}} \sin\theta_{\mathrm{t}}/\lambda}]^{\mathrm{T}} \quad (2)$$

$$\mathbf{b}(\theta_{\mathrm{t}}) \triangleq [1, e^{-j2\pi d_{\mathrm{R}} \sin\theta_{\mathrm{t}}/\lambda}, ..., e^{-j2\pi(N-1)d_{\mathrm{R}} \sin\theta_{\mathrm{t}}/\lambda}]^{\mathrm{T}} \quad (3)$$

$$\mathbf{d}(f_{\mathrm{t}}) \triangleq [1, e^{j2\pi f_{\mathrm{t}}}, ..., e^{j2\pi(L-1)f_{\mathrm{t}}}]^{\mathrm{T}}. \quad (4)$$

with d_{T} and d_{R} being the distances of each two neighboring antenna elements at transmitter and receiver, respectively, and λ being the wavelength.

We assume the clutter range ring is separated into N_{c} patches, which are statistically independent between each other. Moreover, we assume J jamming sources are present, and each jamming is propagated through Q independent paths, including the direct, specular, and diffuse ones. Hence, the observed clutter and jamming signals can be expressed respectively as

$$\mathbf{y}_{\mathrm{c}}(\mathbf{u},\mathbf{S}) = \sum_{i=1}^{N_{\mathrm{c}}} \xi_i(\mathbf{d}(f_i) \odot \mathbf{u}) \otimes (\mathbf{S}^{\mathrm{T}}\mathbf{a}(\theta_i)) \otimes \mathbf{b}(\theta_i) \quad (5)$$

$$\mathbf{y}_{\mathrm{j}} = \sum_{j=1}^{J}\sum_{q=1}^{Q} \beta_{j,q}\boldsymbol{\eta}_{j,q} \otimes \mathbf{b}(\vartheta_{j,q}) \quad (6)$$

where ξ_i is the complex reflection coefficient of the ith clutter patch, $\beta_{j,q}$, $\boldsymbol{\eta}_{j,q} \in \mathbb{C}^{LP\times 1}$, and $\vartheta_{j,q}$ are respectively the complex magnitude, the stacked slow- and fast-time samples, and the spatial angle, all associated with the j-th jamming source scattered through the q-th propagation,

The overall received data vector can be expressed as

$$\mathbf{y}(\mathbf{u},\mathbf{S}) = \mathbf{y}_{\mathrm{t}}(\mathbf{u},\mathbf{S}) + \mathbf{y}_{\mathrm{c}}(\mathbf{u},\mathbf{S}) + \mathbf{y}_{\mathrm{j}} + \mathbf{y}_{\mathrm{n}} \quad (7)$$

where $\mathbf{y}_{\mathrm{n}}$ is the white Gaussian distributed noise vector. Based on (7), the target-free jammer-plus-clutter-plus-noise covariance matrix can be expressed as

$$\begin{aligned}\mathbf{R}_{\mathbf{y}}(\mathbf{u},\mathbf{S}) &\triangleq \mathbb{E}\{\mathbf{y}_{\mathrm{c}}(\mathbf{u},\mathbf{S})\mathbf{y}_{\mathrm{c}}^{\mathrm{H}}(\mathbf{u},\mathbf{S})\} + \mathbb{E}\{\mathbf{y}_{\mathrm{j}}\mathbf{y}_{\mathrm{j}}^{\mathrm{H}}\} + \mathbb{E}\{\mathbf{y}_{\mathrm{n}}\mathbf{y}_{\mathrm{n}}^{\mathrm{H}}\} \\ &\triangleq \mathbf{R}_{\mathrm{c}}(\mathbf{u},\mathbf{S}) + \mathbf{R}_{\mathrm{j}} + \mathbf{R}_{\mathrm{n}} \end{aligned} \quad (8)$$

where the received clutter, jammer, and noise are assumed to be statistically independent, and $\mathbf{R}_{\mathrm{c}}(\mathbf{u},\mathbf{S})$, $\mathbf{R}_{\mathrm{j}}$, and $\mathbf{R}_{\mathrm{n}}$ are their corresponding covariance matrices.

Let $\mathbf{w} \in \mathbb{C}^{NPL\times 1}$ be the adaptive weight vector of the receive filter, $\mathbf{e}_{\mathrm{t}}(\mathbf{u},\mathbf{S}) \triangleq (\mathbf{d}(f_{\mathrm{t}}) \odot \mathbf{u}) \otimes (\mathbf{S}^{\mathrm{T}}\mathbf{a}(\theta_{\mathrm{t}})) \otimes \mathbf{b}(\theta_{\mathrm{t}})$ be the overall steering vector of the target, and $\mathbf{R}_{\mathrm{j+n}} \triangleq \mathbf{R}_{\mathrm{j}} + \mathbf{R}_{\mathrm{n}}$. The output SJCNR of the 3D STAP can be expressed as

$$\mathrm{SJCNR} = \frac{|\alpha_{\mathrm{t}}|^2 \cdot |\mathbf{w}^{\mathrm{H}}\mathbf{e}_{\mathrm{t}}(\mathbf{u},\mathbf{S})|^2}{\mathbf{w}^{\mathrm{H}}\left(\mathbf{R}_{\mathrm{c}}(\mathbf{u},\mathbf{S}) + \mathbf{R}_{\mathrm{j+n}}\right)\mathbf{w}}. \quad (9)$$

Our goal is to maximize the output SJCNR given in (9) in the case of some practical constraints on waveform transmissions. In particular, we seek to find the optimum fast- and slow-time waveforms with good characteristics including constant modulus and certain similarities to quiescent references, so that the SJCNR performance of the MIMO radar STAP can be maximized. Here, we formulate the joint design as follows

$$\begin{aligned} \max_{\mathbf{w},\mathbf{u},\mathbf{S}} \quad & \mathrm{SJCNR} \\ \text{s.t.} \quad & |[\mathbf{S}]_{m,p} - [\mathbf{S}_0]_{m,p}| \le \delta, m = 1,\ldots,M; p = 1,\ldots,P \\ & |\mathbf{u}(l) - \mathbf{u}_0(l)| \le \epsilon, l = 1,\ldots,L \\ & |[\mathbf{S}]_{m,p}| = c_1, m = 1,\ldots,M; p = 1,\ldots,P \\ & |\mathbf{u}(l)| = c_2, l = 1,\ldots,L \\ & |\mathbf{w}^{\mathrm{H}}\mathbf{e}_{\mathrm{t}}(\mathbf{u},\mathbf{S})| = 1 \end{aligned} \quad (10)$$

where $\mathbf{S}_0 \in \mathbb{C}^{M\times P}$ and $\mathbf{u}_0 \in \mathbb{C}^{L\times 1}$ are the quiescent waveform matrix and vector for reference in fast- and slow-time domains, respectively, $\delta > 0$ and $\epsilon > 0$ are parameters of user choice controlling the tolerance on differences between the designed and quiescent waveform references in fast- and slow-time domains, respectively, and c_1 and c_2 are respectively the constant magnitudes of fast- and slow-time waveform elements.

III. Joint Fast- and Slow-Time Waveforms and Receive Filter Design for MIMO STAP

In this section, we first derive the covariance matrices of clutter and jamming signals, based on which we then present a gradient-based approach to solving the joint design via ADMM.

A. Derivations of Covariance Matrices

Introducing $\mathbf{x} \triangleq \mathrm{vec}\{\mathbf{S}^{\mathrm{T}}\} \in \mathbb{C}^{MP\times 1}$, applying the property that $\mathrm{vec}\{\mathbf{ABC}\} = \mathbf{C}^{\mathrm{T}} \otimes \mathbf{A}\mathrm{vec}\{\mathbf{B}\}$ by enabling $\mathbf{A} = \mathbf{I}_P$, $\mathbf{B} = \mathbf{S}^{\mathrm{T}}$, and $\mathbf{C} = \mathbf{a}(\theta_i)$, then (5) can be rewritten as follows

$$\mathbf{y}_{\mathrm{c}}(\mathbf{u},\mathbf{x}) = \sum_{i=1}^{N_{\mathrm{c}}} \xi_i(\mathbf{d}(f_i) \odot \mathbf{u}) \otimes \left(\left(\mathbf{a}^{\mathrm{T}}(\theta_i) \otimes \mathbf{I}_P\right)\mathbf{x}\right) \otimes \mathbf{b}(\theta_i) \quad (11)$$

which can be further derived as

$$\mathbf{y}_{\mathrm{c}}(\mathbf{u},\mathbf{x}) = \sum_{i=1}^{N_{\mathrm{c}}} \xi_i(\mathbf{d}(f_i) \odot \mathbf{u}) \otimes \mathbf{a}^{\mathrm{T}}(\theta_i) \otimes \mathbf{I}_P \otimes \mathbf{b}(\theta_i)\mathbf{x} \quad (12)$$

where the elementary properties of Kronecker product is employed for deriving (11) to (12).

Expanding the Hadamard product in (12), we can further obtain the derivation as follows

$$\mathbf{y}_{\mathrm{c}}(\mathbf{u},\mathbf{x})=\sum_{i=1}^{N_{\mathrm{c}}}\xi_i\mathfrak{D}(\mathbf{d}(f_i))\otimes\left(\mathbf{a}^{\mathrm{T}}(\theta_i)\otimes\mathbf{I}_P\otimes\mathbf{b}(\theta_i)\mathbf{x}\right)\mathbf{u}. \tag{13}$$

Using (8), (12), and (13), the clutter covariance matrix $\mathbf{R}_{\mathrm{c}}(\mathbf{u},\mathbf{x})$ can be obtained as

$$\mathbf{R}_{\mathrm{c}}(\mathbf{u},\mathbf{x})=\sum_{i=1}^{N_{\mathrm{c}}}|\xi_i|^2\mathbf{T}_{\mathbf{x}}(f_i,\theta_i)\mathbf{x}\mathbf{x}^{\mathrm{H}}\mathbf{T}_{\mathbf{x}}^{\mathrm{H}}(f_i,\theta_i) \tag{14}$$

$$=\sum_{i=1}^{N_{\mathrm{c}}}|\xi_i|^2\mathbf{T}_{\mathbf{u}}(f_i,\theta_i)\mathbf{u}\mathbf{u}^{\mathrm{H}}\mathbf{T}_{\mathbf{u}}^{\mathrm{H}}(f_i,\theta_i) \tag{15}$$

where

$$\mathbf{T}_{\mathbf{x}}(f,\theta)\triangleq(\mathbf{d}(f)\odot\mathbf{u})\otimes\mathbf{a}^{\mathrm{T}}(\theta)\otimes\mathbf{I}_P\otimes\mathbf{b}(\theta) \tag{16}$$

$$\mathbf{T}_{\mathbf{u}}(f,\theta)\triangleq\mathfrak{D}(\mathbf{d}(f))\otimes\left(\mathbf{a}^{\mathrm{T}}(\theta)\otimes\mathbf{I}_P\otimes\mathbf{b}(\theta)\mathbf{x}\right). \tag{17}$$

Regarding the covariance matrix of jamming, we deal with the common barrage-noise-type jammers, which are generally mutual independent and Gaussian distributed. Using (6), the jamming covariance matrix can be obtained as

$$\mathbf{R}_{\mathrm{j}}=\sum_{\jmath=1}^{J}\sum_{q=1}^{Q}\sum_{q'=1}^{Q}\beta_{\jmath,q}\beta_{\jmath,q'}^{*}\mathbf{R}_{\jmath,q,q'}^{\boldsymbol{\eta}}\otimes\left(\mathbf{b}(\vartheta_{\jmath,q})\mathbf{b}^{\mathrm{H}}(\vartheta_{\jmath,q'})\right) \tag{18}$$

where $\mathbf{R}_{\jmath,q,q'}^{\boldsymbol{\eta}}\triangleq\mathbb{E}\{\boldsymbol{\eta}_{\jmath,q}\boldsymbol{\eta}_{\jmath,q'}^{\mathrm{H}}\}\in\mathbb{C}^{LP\times LP}$ is the correlation matrix between the jamming signals propagated through the q-th and q'-th paths from the $\jmath$th jamming source.

In addition, the noise covariance matrix $\mathbf{R}_{\mathrm{n}}$ takes the form given by $\mathbf{R}_{\mathrm{n}}=\sigma_{\mathrm{n}}^2\mathbf{I}_{NPL}$.

B. Joint Waveform Synthesis and Adaptive Filter Design

For fixed waveforms $\mathbf{u}$ and $\mathbf{x}$, the design problem (10) reduces to the MVDR optimization problem given as follows

$$\begin{aligned}\max_{\mathbf{w}}\quad&\frac{|\alpha_{\mathrm{t}}|^2|\mathbf{w}^{\mathrm{H}}\mathbf{e}_{\mathrm{t}}(\mathbf{u},\mathbf{x})|^2}{\mathbf{w}^{\mathrm{H}}\mathbf{R}_{\mathrm{c}}(\mathbf{u},\mathbf{x})\mathbf{w}+\mathbf{w}^{\mathrm{H}}\mathbf{R}_{\mathrm{j+n}}\mathbf{w}}\\ \text{s.t.}\quad&|\mathbf{w}^{\mathrm{H}}\mathbf{e}_{\mathrm{t}}(\mathbf{u},\mathbf{x})|=1\end{aligned} \tag{19}$$

whose solution is given by

$$\mathbf{w}=\frac{\left(\mathbf{R}_{\mathrm{c}}(\mathbf{u},\mathbf{x})+\mathbf{R}_{\mathrm{j+n}}\right)^{-1}\mathbf{e}_{\mathrm{t}}(\mathbf{u},\mathbf{x})}{\mathbf{e}_{\mathrm{t}}^{\mathrm{H}}(\mathbf{u},\mathbf{x})\left(\mathbf{R}_{\mathrm{c}}(\mathbf{u},\mathbf{x})+\mathbf{R}_{\mathrm{j+n}}\right)^{-1}\mathbf{e}_{\mathrm{t}}(\mathbf{u},\mathbf{x})}. \tag{20}$$

Stacking $\mathbf{x}$ and $\mathbf{u}$ into a new vector $\boldsymbol{\phi}\triangleq[\mathbf{x}^{\mathrm{T}},\mathbf{u}^{\mathrm{T}}]^{\mathrm{T}}\in\mathbb{C}^{(MP+L)\times1}$, inserting (20) into (9), then we can rewrite the design problem (10) into the form as follows

$$\begin{aligned}\min_{\boldsymbol{\phi}}\quad&-\mathbf{e}_{\mathrm{t}}^{\mathrm{H}}(\boldsymbol{\phi})\left(\mathbf{R}_{\mathrm{c}}(\boldsymbol{\phi})+\mathbf{R}_{\mathrm{j+n}}\right)^{-1}\mathbf{e}_{\mathrm{t}}(\boldsymbol{\phi})\\ \text{s.t.}\quad&|\boldsymbol{\phi}(r)-\boldsymbol{\phi}_0(r)|\le\begin{cases}\delta,\ r=1,\ldots,MP\\ \epsilon,\ \text{otherwise}\end{cases}\\ &|\boldsymbol{\phi}(r)|=\begin{cases}c_1,\ r=1,\ldots,MP\\ c_2,\ \text{otherwise}\end{cases}\end{aligned} \tag{21}$$

where $\boldsymbol{\phi}_0\triangleq[(\mathrm{vec}\{\mathbf{S}_0\})^{\mathrm{T}},\mathbf{u}_0^{\mathrm{T}}]^{\mathrm{T}}\in\mathbb{C}^{(MP+L)\times1}$.

To solve (21), we introduce a virtually auxiliary vector $\mathbf{z}\in\mathbb{C}^{MPL\times1}$ to add an additional constraint, i.e., $\boldsymbol{\phi}=\mathbf{z}$. Therefore, the optimization problem (21) can be transformed into the form as follows

$$\begin{aligned}\min_{\boldsymbol{\phi},\mathbf{z}}\quad&-\mathbf{e}_{\mathrm{t}}^{\mathrm{H}}(\boldsymbol{\phi})\left(\mathbf{R}_{\mathrm{c}}(\boldsymbol{\phi})+\mathbf{R}_{\mathrm{j+n}}\right)^{-1}\mathbf{e}_{\mathrm{t}}(\boldsymbol{\phi})\\ \text{s.t.}\quad&|\mathbf{z}(r)-\boldsymbol{\phi}_0(r)|\le\begin{cases}\delta,\ r=1,\ldots,MP\\ \epsilon,\ \text{otherwise}\end{cases}\\ &|\mathbf{z}(r)|=\begin{cases}c_1,\ r=1,\ldots,MP\\ c_2,\ \text{otherwise}\end{cases}\\ &\boldsymbol{\phi}=\mathbf{z}\end{aligned} \tag{22}$$

to which the ADMM framework [18] can be applied for finding its solutions.

Note that the objective function of (22) is difficult to handle. To tackle it, we use its first-order Taylor expansion at the point $\boldsymbol{\phi}^{(k)}$ obtained after the kth iteration to construct the approximated augmented Lagrangian [19] of (22) given by

$$\mathcal{L}(\boldsymbol{\phi},\mathbf{z},\boldsymbol{\lambda})=\mathcal{F}(\boldsymbol{\phi}^{(k)})+\left(\nabla^{(k)}\mathcal{F}(\boldsymbol{\phi})\right)^{\mathrm{H}}\boldsymbol{\phi}+\boldsymbol{\lambda}^{\mathrm{H}}(\boldsymbol{\phi}-\mathbf{z})+\rho\|\boldsymbol{\phi}-\mathbf{z}\|^2 \tag{23}$$

where $\mathcal{F}(\boldsymbol{\phi})\triangleq-\mathbf{e}_{\mathrm{t}}^{\mathrm{H}}(\boldsymbol{\phi})\left(\mathbf{R}_{\mathrm{c}}(\boldsymbol{\phi})+\mathbf{R}_{\mathrm{j+n}}\right)^{-1}\mathbf{e}_{\mathrm{t}}(\boldsymbol{\phi})$, $\boldsymbol{\lambda}\in\mathbb{C}^{MPL\times1}$ is the Lagrangian multiplier vector, and $\rho>0$ is the penalty parameter. Based on this, we can rewrite (22) as

$$\begin{aligned}\min_{\boldsymbol{\phi},\mathbf{z},\boldsymbol{\lambda}}\quad&\mathcal{L}\left(\boldsymbol{\phi},\mathbf{z},\boldsymbol{\lambda}\right)\\ \text{s.t.}\quad&|\mathbf{z}(r)-\boldsymbol{\phi}_0(r)|\le\begin{cases}\delta,\ r=1,\ldots,MP\\ \epsilon,\ \text{otherwise}\end{cases}\\ &|\mathbf{z}(r)|=\begin{cases}c_1,\ r=1,\ldots,MP\\ c_2,\ \text{otherwise}\end{cases}.\end{aligned} \tag{24}$$

Note that the first component of the Lagrangian (23) is constant, which is immaterial to optimization, while the second component of (23), denoted by ς, can be expanded as follows

$$\varsigma\triangleq\left(\nabla^{(k)}\mathcal{F}(\boldsymbol{\phi})\right)^{\mathrm{H}}\boldsymbol{\phi}=\left(\boldsymbol{\upsilon}_{\mathbf{x}}^{(k)}\right)^{\mathrm{H}}\mathbf{x}+\left(\boldsymbol{\upsilon}_{\mathbf{u}}^{(k)}\right)^{\mathrm{H}}\mathbf{u}+\mathrm{const.} \tag{25}$$

where $\boldsymbol{\upsilon}_{\mathbf{x}}$ and $\boldsymbol{\upsilon}_{\mathbf{u}}$ are respectively defined as

$$\begin{aligned}\boldsymbol{\upsilon}_{\mathbf{x}}\triangleq&-2\mathbf{T}_{\mathbf{x}}^{\mathrm{H}}(f_{\mathrm{t}},\theta_{\mathrm{t}})\boldsymbol{\Omega}\mathbf{T}_{\mathbf{x}}(f_{\mathrm{t}},\theta_{\mathrm{t}})\mathbf{x}+2\sum_{i=1}^{N_{\mathrm{c}}}|\xi_i|^2\mathbf{T}_{\mathbf{x}}^{\mathrm{H}}(f_i,\theta_i)\\ &\times\boldsymbol{\Omega}^{\mathrm{H}}\mathbf{T}_{\mathbf{x}}(f_{\mathrm{t}},\theta_{\mathrm{t}})\mathbf{x}\mathbf{x}^{\mathrm{H}}\mathbf{T}_{\mathbf{x}}^{\mathrm{H}}(f_{\mathrm{t}},\theta_{\mathrm{t}})\boldsymbol{\Omega}\mathbf{T}_{\mathbf{x}}(f_i,\theta_i)\mathbf{x}\end{aligned} \tag{26}$$

$$\begin{aligned}\boldsymbol{\upsilon}_{\mathbf{u}}\triangleq&-2\mathbf{T}_{\mathbf{u}}^{\mathrm{H}}(f_{\mathrm{t}},\theta_{\mathrm{t}})\boldsymbol{\Omega}\mathbf{T}_{\mathbf{u}}(f_{\mathrm{t}},\theta_{\mathrm{t}})\mathbf{u}+2\sum_{i=1}^{N_{\mathrm{c}}}|\xi_i|^2\mathbf{T}_{\mathbf{u}}^{\mathrm{H}}(f_i,\theta_i)\\ &\times\boldsymbol{\Omega}^{\mathrm{H}}\mathbf{T}_{\mathbf{u}}(f_{\mathrm{t}},\theta_{\mathrm{t}})\mathbf{u}\mathbf{u}^{\mathrm{H}}\mathbf{T}_{\mathbf{u}}^{\mathrm{H}}(f_{\mathrm{t}},\theta_{\mathrm{t}})\boldsymbol{\Omega}\mathbf{T}_{\mathbf{u}}(f_i,\theta_i)\mathbf{u}\end{aligned} \tag{27}$$

with $\boldsymbol{\Omega}\triangleq(\mathbf{R}_{\mathrm{c}}(\mathbf{u},\mathbf{x})+\mathbf{R}_{\mathrm{j+n}})^{-1}$.

Till now, we can first apply the standard ADMM procedures to solve the unconstrained version of (24), together with the formulated Lagrangian (23). Then, we enforce a proper projection to its feasibility set in terms of constraints that are maintained. Here, at the $(k+1)$-th iteration, the resulting ADMM update for (24) in terms of the variable $\mathbf{z}$ after

Algorithm 1 3D Joint Design Algorithm.

1: Initialization: $\mathbf{z}^{(0)}, \boldsymbol{\phi}^{(0)}, \boldsymbol{\lambda}^{(0)}, \rho, k \leftarrow 0$
2: **repeat**
3: Construct $\mathbf{T}_{\mathbf{x}}^{(k)}$ and $\mathbf{T}_{\mathbf{u}}^{(k)}$ via (16) and (17)
4: Calculate $\boldsymbol{\upsilon}_{\mathbf{x}}^{(k)}$ and $\boldsymbol{\upsilon}_{\mathbf{u}}^{(k)}$ via (26) and (27)
5: Update $\mathbf{z}$, $\boldsymbol{\phi}$, and $\boldsymbol{\lambda}$ via (28), (31), and (32)
6: $k \leftarrow k+1$
7: **until** convergence
8: Recover $\mathbf{S}$ and $\mathbf{u}$ from $\boldsymbol{\phi}$
9: Calculate $\mathbf{w}$ via (20)

projection can be expressed as [13]

$$\mathbf{z}^{(k+1)}(r)=\boldsymbol{\kappa}(r)\begin{cases} e^{j\boldsymbol{\tau}^{(k)}(r)}, \ \boldsymbol{\tau}^{(k)}(r)\in[\boldsymbol{\gamma}(r),\boldsymbol{\gamma}(r)+\boldsymbol{\sigma}(r)] \\ e^{j\boldsymbol{\gamma}(r)}, \ \boldsymbol{\tau}^{(k)}(r)\in[\boldsymbol{\gamma}(r)+\frac{\boldsymbol{\sigma}(r)}{2}-\pi,\boldsymbol{\gamma}(r)] \\ e^{j(\boldsymbol{\gamma}(r)+\boldsymbol{\sigma}(r))}, \ \text{otherwise} \end{cases} \tag{28}$$

where $\boldsymbol{\tau} \triangleq \arg(\boldsymbol{\phi}+\frac{1}{2\rho}\boldsymbol{\lambda})$, $\boldsymbol{\kappa}(r)=\begin{cases} c_1, r=1,\ldots,MP \\ c_2, \text{otherwise} \end{cases}$, and

$$\boldsymbol{\gamma}(r)=\begin{cases} \arg(\boldsymbol{\phi}_0(r))-\arccos(1-\delta^2/2), r=1,\ldots,MP \\ \arg(\boldsymbol{\phi}_0(r))-\arccos(1-\epsilon^2/2), \text{otherwise} \end{cases} \tag{29}$$

$$\boldsymbol{\sigma}(r)=\begin{cases} 2\arccos(1-\delta^2/2), r=1,\ldots,MP \\ 2\arccos(1-\epsilon^2/2), \text{otherwise} \end{cases}. \tag{30}$$

Similarly, the ADMM update for (24) in terms of $\boldsymbol{\phi}$ can be expressed in the form given as follows

$$\boldsymbol{\phi}^{(k+1)} = \mathbf{z}^{(k+1)} - \frac{1}{2\rho}\left(\boldsymbol{\lambda}^{(k)} + \left[(\boldsymbol{\upsilon}_{\mathbf{x}}^{(k)})^{\mathrm{T}}, (\boldsymbol{\upsilon}_{\mathbf{u}}^{(k)})^{\mathrm{T}}\right]^{\mathrm{T}}\right) \tag{31}$$

and the update of the Lagrangian multiplier vector is given by

$$\boldsymbol{\lambda}^{(k+1)} = \boldsymbol{\lambda}^{(k)} + 2\rho\left(\boldsymbol{\phi}^{(k+1)} - \mathbf{z}^{(k+1)}\right). \tag{32}$$

The overall procedures for the joint design are summarized in Algorithm 1, for which the Steffensen-type acceleration [20] with fixed-point iterations can be applied.

IV. Simulation Results

In this section, we evaluate the performances of our proposed algorithm, including the SJCNR convergence and similarity performances. We consider a colocated MIMO radar equipped with $M = 2$ transmit and $N = 3$ receive antenna elements spaced half-wavelength apart from each other, which emits $L = 5$ pluses in one radar CPI. The fast-time code length of waveforms is set to be $P = 128$. We assume the target is located at $\theta_{\mathrm{t}} = 20^{\circ}$ with a normalized Doppler frequency $f_{\mathrm{t}} = 0.35$, whose initial signal-to-noise ratio is SNR $= 10$ dB. In total, there are $N_{\mathrm{c}} = 10$ clutter patches uniformly distributing within the spatial range $[-90^{\circ}, 90^{\circ}]$, and there are $J = 2$ independent barrage-noise-type jammers propagating through $Q = 2$ paths. All jamming signals and their spatial directions are randomly generated. We choose spectrally-agile waveforms whose stop-bands of power spectral density (PSD) are set to be $[0.5\pi, 0.75\pi] \cup [1.25\pi, 1.5\pi]$ as the fast-time quiescent references, and choose unimodular random sequences as the slow-time references. The constant magnitudes are set to be $c_1 = c_2 = 1$.

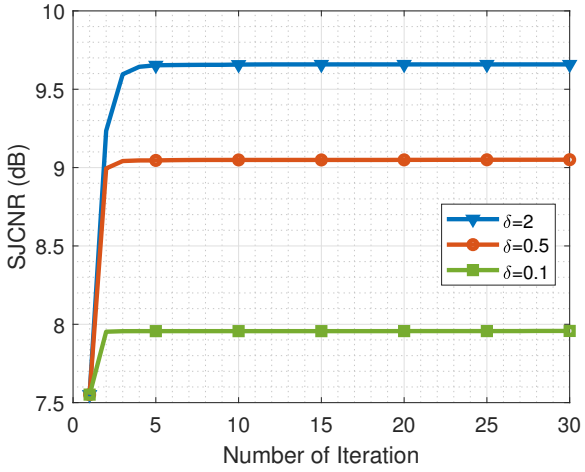

Fig. 1: SJCNR performance versus the number of iterations.

Example 1: SJCNR Convergence Evaluation. We evaluate the obtained SJCNR performance versus the number of iterations. The tolerance parameter for fast-time waveform approximation is set to be $\delta = 0.1$, 0.5, and 2 (corresponding to the similarity-free case [13]), while the slow-time similarity is assumed to be secondary, whose tolerance parameter is set to be $\epsilon = 2$.

It can be seen from Fig. 1 that the proposed algorithm shows good convergence speed for all the three cases tested in this example, which verifies its capability on clutter and jammer suppression. After 5 iterations, the SJCNR for the similarity-free case ($\delta = 2$) has reached 9.66 dB, while the SJCNRs for the other two tested cases ($\delta = 0.1$ and 0.5) has reached 7.96 dB and 9.05 dB, respectively. It can also be seen that the SJCNR under the most strict constraint (i.e., $\delta = 0.1$) improves only 0.41 dB compared to the initial SJCNR before optimization. This means a strict similarity constraint leads to a poor SJCNR performance, and a trade-off between the SJCNR performance and the similarity to reference waveforms is normally made.

Example 2: Similarity Performance Evaluation. We evaluate the similarity performance of the proposed algorithm, wherein we show the normalized PSD approximation of the two designed fast-time waveforms to their references (marked as 'Ref 1' and 'Ref 2'). The PSD level of the reference waveforms in stop-bands is around -45 dB on average, and the worst spectral attendation is -39.65 dB. Here, a lower level of PSD in the stop-bands means a higher similarity to the references.

It can be seen from Fig. 2 that all the designed waveforms show low PSD levels in the stop-bands, meaning that the proposed algorithm has met the condition of similarity constraints. For the first waveform reference, it can be seen from Fig. 2(a) that the maximum, minimum, and average PSD levels in stop-bands for $\delta = \{0.1, 0.5\}$ are around $\{-10.40, -21.47\}$ dBs, $\{-37.57, -49.54\}$ dBs, and

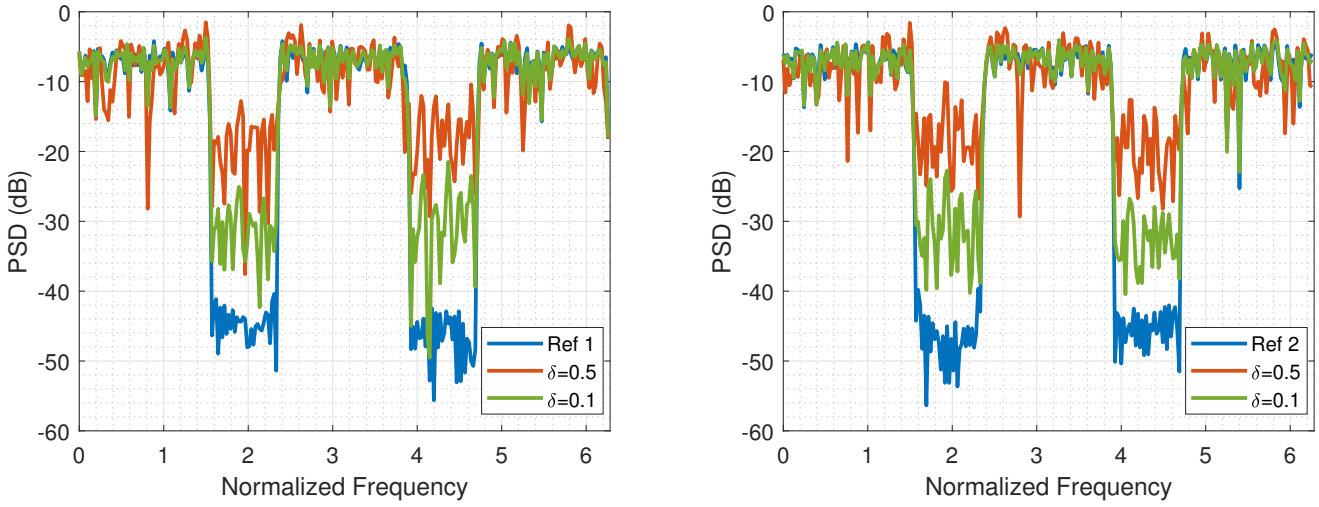

(a) PSD of the first waveform.

(b) PSD of the second waveform.

Fig. 2: PSDs of two designed fast-time waveforms for MIMO radar and their references.

$\{-20, -35\}$ dBs, respectively. For the second waveform reference, it can be seen from Fig. 2(b) that the maximum, minimum, and average PSD levels obtained in stop-bands for $\delta = \{0.1, 0.5\}$ are around $\{-10.08, -22.71\}$ dBs, $\{-28.22, -40.43\}$ dBs, and $\{-20, -35\}$ dBs, respectively.

V. Conclusion

We have studied the problem of jointly designing transmit waveforms and receive filter for the 3D STAP of MIMO radar, which deals with the complex environment where both clutter and jamming signals are present. Both fast-time waveforms and slow-time coding among pulses have been considered in the joint design. To be specific, we have maximized the SJCNR at the output, and have also guaranteed the constant-modulus and similarity constraints for the waveform transmission. A non-convex optimization problem has been formulated, which has been then recast into a form that allows the application of ADMM for finding solutions. An algorithm has been proposed for the joint design problem, whose effectiveness has been verified by simulations.

References

[1] J. Li and P. Stoica, "MIMO radar with colocated antennas," *IEEE Signal Process. Mag.*, vol. 24, no. 5, pp. 106–114, Sep. 2007.

[2] H. He, J. Li, and P. Stoica, *Waveform design for active sensing systems: A computational approach*. Cambridge University Press, 2012.

[3] D. W. Bliss and K. W. Forsythe, "Multiple-input multiple-output (MIMO) radar and imaging: Degrees of freedom and resolution," in *Proc. Asilomar Conf. Signals, Syst., Comput.*, vol. 1, Pacific Grove, CA, USA, Nov. 2003, pp. 54–59.

[4] H. Hao, P. Stoica, and J. Li, "Designing unimodular sequences sets with good correlations—Including an application to MIMO radar," *IEEE Trans. Signal Process.*, vol. 57, no. 11, pp. 4391–4405, Nov. 2009.

[5] Y. Li and S. A. Vorobyov, "Fast algorithms for designing multiple unimodular waveforms with good correlation properties," *IEEE Trans. Signal Process.*, vol. 66, no. 5, pp. 1197–1212, Mar. 2018.

[6] C.-Y. Chen and P. P. Vaidyanathan, "MIMO radar space-time adaptive processing using prolate spheroidal waveform functions," *IEEE Trans. Signal Process.*, vol. 56, no. 2, pp. 623–635, Feb. 2008.

[7] Y. Li, S. A. Vorobyovz, and Z. He, "Joint hot and cold clutter mitigation in the transmit beamspace-based MIMO radar," in *Proc. Int. Conf. Acoust. Speech, Signal Process. (ICASSP)*, 2015, pp. 2334–2338.

[8] Y. Li, S. A. Vorobyov, and Z. He, "Terrain-scattered jammer suppression in MIMO radar using space-(fast) time adaptive processing," in *Proc. Int. Conf. Acoust. Speech, Signal Process. (ICASSP)*, 2016, pp. 3026–3033.

[9] S. Jardak, S. Ahmed, and M.-S. Alouini, "Generation of correlated finite alphabet waveforms using Gaussian random variables," *IEEE Trans. Signal Process.*, vol. 62, no. 17, pp. 4587–4596, Sep. 2014.

[10] D. R. Fuhrmann and G. San Antonio, "Transmit beamforming for MIMO radar systems using signal cross-correlation," *IEEE Trans. Aerosp. Electron. Syst.*, vol. 44, no. 1, pp. 171–186, 2008.

[11] A. Hassanien and S. A. Vorobyov, "Transmit energy focusing for DOA estimation in MIMO radar with colocated antennas," *IEEE Trans. Signal Process.*, vol. 59, no. 6, pp. 2669–2682, Jun. 2011.

[12] P. Stoica, J. Li, and M. Xue, "Transmit codes and receive filters for radar," *IEEE Signal Process. Mag.*, vol. 25, no. 6, pp. 94–109, Nov. 2008.

[13] A. De Maio, S. D. Nicola, Y. Huang, Z.-Q. Luo, and S. Zhang, "Design of phase codes for radar performance optimization with a similarity constraint," *IEEE Trans. Signal Process.*, vol. 57, no. 2, pp. 610–621, Feb. 2009.

[14] A. Aubry, A. De Maio, A. Farina, and M. Wicks, "Knowledge-aided (potentially cognitive) transmit signal and receive filter design in signal-dependent clutter," *IEEE Trans. Aerosp. Electron. Syst.*, vol. 49, no. 1, pp. 93–117, Jan. 2013.

[15] G. Cui, X. Yu, V. Carotenuto, and L. Kong, "Space-time transmit code and receive filter design for colocated MIMO radar," *IEEE Trans. Signal Process.*, vol. 65, no. 5, pp. 1116–1129, Mar. 2017.

[16] Y. Li and S. Vorobyov, "Joint space-(slow) time transmission with unimodular waveforms and receive adaptive filter design for radar," in *Proc. Int. Conf. Acoust. Speech, Signal Process. (ICASSP)*, 2018, pp. 3276–3280.

[17] X. Yu, K. Alhujaili, G. Cui, and V. Monga, "MIMO radar waveform design in the presence of multiple targets and practical constraints," *IEEE Trans. Signal Process.*, vol. 68, pp. 1974–1989, Mar. 2020.

[18] S. Boyd, N. Parikh, E. Chu, B. Peleato, and J. Eckstein, *Distributed Optimization and Statistical Learning via the Alternating Direction Method of Multipliers*. Delft, The Netherlands: now Publisher Inc., Jan. 2011.

[19] H. Ouyang, N. He, L. Tran, and A. Gray, "Stochastic alternating direction method of multipliers," in *Proc. Int. Conf. Machine Learning*, Jun. 2013, pp. 80–88.

[20] A. Cordero, J. L. Hueso, E. Martínez, and J. R. Torregrosa, "Steffensen type methods for solving nonlinear equations," *J. Comput. Appl. Math.*, vol. 236, pp. 3058–3064, Jun. 2012.